(2)

NRL Memorandum Report 5254

AD A139364

Variations of Structural Response to Underwater Explosion with Charge Standoff and Unsymmetric Loading

W. W. WEBBON

Structural Integrity Branch
Marine Technology Division

March 6, 1984

NAVAL RESEARCH LABORATORY
Washington, D.C.

84 03 22 127

REPORT DOCUMENTATION PAGE

1a. REPORT SECURITY CLASSIFICATION UNCLASSIFIED	1b. RESTRICTIVE MARKINGS
2a. SECURITY CLASSIFICATION AUTHORITY	3. DISTRIBUTION/AVAILABILITY OF REPORT Approved for public release; distribution unlimited.
2b. DECLASSIFICATION/DOWNGRADING SCHEDULE	
4. PERFORMING ORGANIZATION REPORT NUMBER(S) NRL Memorandum Report 5254	5. MONITORING ORGANIZATION REPORT NUMBER(S)
6a. NAME OF PERFORMING ORGANIZATION Naval Research Laboratory 6b. OFFICE SYMBOL (If applicable)	7a. NAME OF MONITORING ORGANIZATION
6c. ADDRESS (City, State and ZIP Code) Washington, DC 20375	7b. ADDRESS (City, State and ZIP Code)
8a. NAME OF FUNDING/SPONSORING ORGANIZATION David Taylor Naval Ship R&D Center 8b. OFFICE SYMBOL (If applicable)	9. PROCUREMENT INSTRUMENT IDENTIFICATION NUMBER
8c. ADDRESS (City, State and ZIP Code) Bethesda, MD 20084	10. SOURCE OF FUNDING NOS. PROGRAM ELEMENT NO. / PROJECT NO. / TASK NO. / WORK UNIT NO. 58-0268-0-3
11. TITLE (Include Security Classification) (See page ii)	
12. PERSONAL AUTHOR(S) W. W. Webbon	
13a. TYPE OF REPORT Interim 13b. TIME COVERED FROM _____ TO _____	14. DATE OF REPORT (Yr., Mo., Day) March 6, 1984 15. PAGE COUNT 25
16. SUPPLEMENTARY NOTATION	

17. COSATI CODES			18. SUBJECT TERMS (Continue on reverse if necessary and identify by block number)
FIELD	GROUP	SUB. GR.	Structural dynamics; Multifoundation; Dynamic design; Submarines; Shipboard shock

19. ABSTRACT (Continue on reverse if necessary and identify by block number)

This interim report summarizes results obtained in conjunction with continuing work toward extension of the Navy's Dynamic Design Analysis Method (DDAM) to multiple foundation motion. A dynamic model of a hull section containing simulated internal equipment with two supports was analyzed using the Variable Geometry Submarine Model (VGSM) for response to underwater explosions with varying charge standoffs. Charge weights were also varied such that the shock factor component normal to the hull was maintained constant for each standoff. Both symmetric and unsymmetric charge geometries with respect to the simulated equipment were examined. Results show that there is a trend toward reduced severity of shock predicted by this simulation for this equipment as the standoff is increased for constant shock factor. The unsymmetric loading resulting in different foundation motions of the two equipment supports shows a trend toward reduced severity of shock for many locations when the foundation motions are uncorrelated (small standoff). However, some locations, particularly those excited by unsymmetric modes of vibration, experience a significant increase in severity. As the unsymmetric charge geometry becomes more approximately symmetric for larger standoffs, the foundation motions become more correlated and the shock response approaches the symmetric case.

20. DISTRIBUTION/AVAILABILITY OF ABSTRACT UNCLASSIFIED/UNLIMITED ☒ SAME AS RPT. ☐ DTIC USERS ☐	21. ABSTRACT SECURITY CLASSIFICATION UNCLASSIFIED
22a. NAME OF RESPONSIBLE INDIVIDUAL W. W. Webbon	22b. TELEPHONE NUMBER (Include Area Code) (202) 767-3613 22c. OFFICE SYMBOL Code 5831

DD FORM 1473, 83 APR EDITION OF 1 JAN 73 IS OBSOLETE.

11. TITLE

VARIATIONS OF STRUCTURAL RESPONSE TO UNDERWATER EXPLOSION WITH CHARGE STANDOFF AND UNSYMMETRIC LOADING

CONTENTS

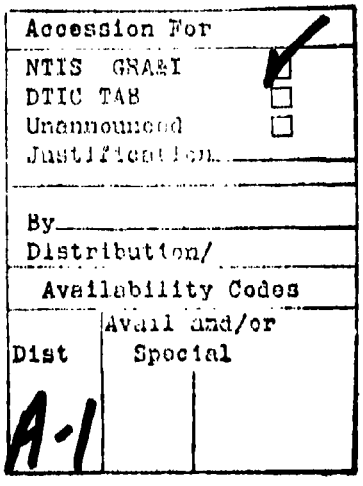

VARIATIONS OF STRUCTURAL RESPONSE TO UNDERWATER EXPLOSION WITH CHARGE STANDOFF AND UNSYMMETRIC LOADING

INTRODUCTION

This interim report summarizes results obtained in conjunction with continuing work toward extension of the Navy's Dynamic Design Analysis Method (DDAM) to multiple foundation motion. A dynamic model of a hull section containing simulated internal equipment with two supports was analyzed using the Variable Geometry Submarine Model (VGSM) for response to underwater explosions with varying charge standoffs. Charge weights were also varied such that the shock factor component normal to the hull was maintained constant for each standoff. Both symmetric and unsymmetric charge geometries with respect to the simulated equipment were examined. Results show that there is a trend toward reduced severity of shock predicted by this simulation for this equipment as the standoff is increased for constant shock factor. The unsymmetric loading resulting in different foundation motions of the two equipment supports shows a trend toward reduced severity of shock for many locations when the foundation motions are uncorrelated (small standoff). However, some locations, particularly, those excited by unsymmetric modes of vibration, experience a significant increase in severity. As the unsymmetric charge geometry becomes more approximately symmetric for larger standoffs, the foundation motions become more correlated and the shock response approaches the symmetric case. Acknowledgement to Mr. G. J. O'Hara is extended for his original assistance and inspiration in the development of this study and analysis method.

BACKGROUND

Use of the VGSM program in combination with an internal equipment model to simulate response to an underwater explosion is summarized in [1]. Figures 1 through 3 display, respectively, the VGSM model, the internal equipment model and the subset of fixed base modes and frequencies of the internal equipment model used in this study. Figure 4 illustrates the symmetric and unsymmetric loading geometries used in the simulation, identified as Case A and Case B, respectively. The shock factor component normal to the hull at foundation 18 is maintained a constant for both geometries as the charge weight and standoff are varied for six standoff values. A time history length of 40 ms was used to obtain all responses. Reference [1] contains a verification of the numerical accuracy of computing internal equipment responses using VGSM as compared to very accurate modal superposition calculations. Reference [2] contains information concerning VGSM, version III methodology. It must be emphasized that the numerical techniques for calculation of underwater shock response by VGSM (and probably any other method) are subject to error due to many unknowns. Results are indicative of trends only, and must be verified by tests. Points of curves in plots of structure response in this report use spline interpolation primarily for the sake of visualization of trends. Many of the quantities which are displayed may be expected to have a random character which cannot be adequately shown without considerably more

Manuscript approved November 28, 1983.

standoff data points. Note, that for convenience in plotting, the standoff values for Case A were used for both Cases A and B. The standoff values for these cases are virtually the same for plotting purposes except perhaps for the smallest standoff (4.9m versus 5.6m).

VARIATION OF RESPONSE WITH STANDOFF

A measure of the variation of response with standoff is the variation of the peak kinetic, potential, and total energies achieved by the structure as a function of each standoff. The simulated equipment model kinetic energy is calculated for each point in time from the summation of the kinetic energies of all of the masses, m_i, having absolute velocities, z_i, from[3]

$$K.E. = \frac{1}{2} \sum_{i=1}^{16} m_i \dot{z}_i^2 \qquad (1)$$

The potential energy is due to the elastic strain energy of the simulated equipment model and is calculated from the relation[3]

$$P.E. = \frac{1}{2} \sum_{i}^{18} \sum_{j}^{18} z_i K_{ij} z_j \qquad (2),$$

where z_i is the absolute displacement of m_i and K_{ij} is the stiffness component in direction i due to displacement in direction j.

The three energy quantities are plotted in Figs. 5, 6, and 7 for both Case A and Case B. These quantities consider only energy within the simulated equipment. It is apparent that a significant reduction in the energy input to the structure has occurred with increasing standoff as determined through this simulated explosion with the VGSM program.

For comparison purposes, Figs. 8 through Fig. 11 illustrate the overpressure, the time constant, energy per unit area, and the impulse per unit area of the explosion at the hull, respectively. These quantities were calculated using equations 6.12, 6.13, 6.14, 6.15 of reference [5].

The large differences in the pressure, energy and impulse curves for the 4.9m Case A standoff versus the 5.6m Case B standoff are due to the sensitivity of these quantities to the standoff values. The calculations are made for the point normal to the hull and closest to the explosion. Case A, being closer to the hull and centrally located with respect to the equipment will result in greater loading of the equipment. This is the tradeoff which results from maintaining the component of shock factor normal to the hull at node 18 as a constant for both cases. This tradeoff explains the rapid increase in the energy for the first standoff for Case A. The rapid decrease of the energy for Case B may be due to unsymmetric loading effects, discussed later.

The peak modal amplitudes for the absolute accelerations for Case A are plotted versus standoff in Fig. 12. These accelerations are indicators of the dynamic forces. The largest accelerations, due to mode 6, are seen to decrease slowly as the standoff increases to 22m and thereafter to decrease more rapidly. For mode 3, the accelerations increase with standoff, while for modes 1 and 5 slow reduction with standoff occurs. Hence, the general trend

toward reduced response with standoff indicated by the energy plots is corroborated by this acceleration plot with the exception that an increase did occur for one of the modes examined.

VARIATION OF RESPONSE WITH UNSYMMETRIC LOADING

Peak absolute values of simulated equipment structure moments are plotted versus standoff for various locations in Figs. 13 through Fig. 15. Bending moments number 1, 2, and 3, refer to nodes 4, 6, and 14 of the equipment model, respectively. Bending moment #1 is higher for the unsymmetric loading. This is probably because unsymmetric modes are excited and contribute moment at node 4 controlling this response. Note the relatively gentle increase in slope as standoff is reduced for bending moment #1. This implies that as standoff is reduced, the unsymmetric modes, which are always being excited for Case B, become, smoothly, more significant. However, in Fig. 14, there is a sudden reduction for bending moment #2 at the 5.6m Case B standoff. This moment is dominated by symmetric modes and the sudden reduction may be due to reduced excitation of the symmetric modes because of the pronounced unsymmetric loading. Bending moment #3 appears to be a mix between the two being farther from the supports and less sensitive to the input motions. The approximately equal responses for larger standoffs imply that the foundation motions due to the unsymmetric shot are correlated and rapidly approach the symmetric case. This correlation phenomenon was further examined by plotting the normalized correlation coefficients [3,4] of the motions of foundation nodes 17 and 18 versus standoff (Fig. 16). The improved correlation with standoff is clear from these plots. The abrupt change in moment response is accompanied by an increase in the correlation of the velocities and accelerations. A similar abrupt change also occurs for the energy plots and occurs in other responses as well. It should be noted that the apparently lower responses for Case B for the closest standoff for symmetrically excited locations are dependent upon the simulated equipment. A statically indeterminant simulated equipment item might experience high loading due to differential motions of the foundations, for example. The simulated equipment model used in this simulation is statically determinant and no additional stresses are induced statically due to differential motions.

A possible amplification of the response due to unsymmetric loading could occur if the time delay of the loading at node 17 were calculated as a half period of the dominant mode of the response. This possibility with respect to response of suspension bridges is discussed in references [6], [7], and [8]. Hasselman shows in [8] that an amplification as high as a factor of 2 may occur in an idealized case. A geometric configuration intended to test this possibility should be included in further studies.

ADDITIONAL EXAMPLES OF TRENDS TOWARD REDUCED RESPONSE WITH STANDOFF

Figure 17 through Figure 22 illustrate the variation of equipment spring forces and reactions. In most cases, there is a trend toward marked reduction in shock severity with standoff. The exceptions occur primarily for internal spring forces between the two beams of the simulated equipment. A modest increase in response occurs for Case A out to 22m for the supporting springs. Hence, it is important to note that there are some particular

locations where peak internal forces increase slightly with standoff as predicted by this VGSM simulation. Figure 23 through Figure 25 illustrate the variation of the equipment including the mass of the VGSM structure at the support points. These figures are included for comparison and checking purposes. Figure 23 displays the peak value of the sum of the $m_i \ddot{z}_i$ terms for each standoff for Cases A and B. This is the sum of all dynamic loads delivered to the equipment structure including the hull mass at the support points and may also be viewed as the peak reaction force of the structure. This may be compared to Fig. 21 which is equivalent to Fig. 23 except VGSM masses have not been included. Hence, the VGSM mass responses predominate. Figure 24 illustrates the correlation of Case A and Case B as Case B geometry more nearly approximates that of Case A with increasing standoff. Figure 25 verifies that the shock factor has been maintained constant at node 18. Figures 26 through 30 illustrate the variation of accelerations at important points on the equipment model. As already mentioned, spline interpolation is included for visualization. As these quantities may vary significantly between the values of standoff calculated, significantly more values would be required to more accurately characterize the motion. Figure 26 shows a general trend toward reduction with standoff with the exception of an increase in response at 22m standoff for Case A. Figure 27 shows that the acceleration at the unsymmetrically excited location of mass 4 is usually higher for Case B. After an initial reduced response at 12m, the response is, approximately, constant thereafter. In Figure 28, mass #6 experiences the same character of response as bending moment #2 in Fig. 14. In Figure 29, Case B predominates. Finally, the response of mass 14 in Fig. 30 is very similar to that of bending moment #3 in Fig. 15.

CONCLUSIONS:

1. For symmetric loading, Case A, small increases in response with increasing standoff are predicted in Figs. 17, 18, 19, 20, 22, and in Fig. 12 for mode 3. For most other responses, for Case A, large decreases in response and in equipment energy are predicted. Therefore, the simulation predicts a trend toward reduced response with standoff for symmetric loading of this symmetric structure.

2. Considering the envelope of both Case A and Case B responses, small increases in structural response or energy occur in Figs. 5, 12, 15, 17, 18, 19, 20 and 21. For most other responses, large decreases are predicted as standoff is increased. Therefore the simulation also predicts a trend toward reduced response with standoff when the envelope of responses for both Case A and Case B is considered.

3. For unsymmetric loading, Case B, significant increases in response above those predicted for symmetric loading are predicted in Figs. 13, 19, 20, 22, 26, 27, and 29. Most of these locations are locations where unsymmetric modes contribute to the response. The largest of these is shown in Fig. 27 where the acceleration of mass 4 is 72% higher than that predicted for the 22m standoff for Case A. Therefore, the simulation predicts that responses due to unsymmetric loading can be higher than those due to symmetric loading. This

suggests that unsymmetric loadings should be considered in design calculations.

4. For highly unsymmetric loading and little correlation of the input foundation motions, locations which are normally dominated by symmetric modes show a trend toward reduced response with decorrelation. For locations which are dominated by unsymmetric modes, however, decorrelation does not usually reduce the response.

REFERENCES

1. W. W. Webbon, G. J. O'Hara, "Toward a Multifoundation Dynamic Design Analysis Method," NRL Memorandum Rept. 4800, Naval Research Laboratory, May 19, 1982. ADB 064710L

2. B. C. McNaight, "The Variable Geometry Submarine Model (VGSM), Version III, Users Manual," M & T Rept. No. A790902, The M&T Company, September 1979.

3. W. T. Thomson, Theory of Vibration with Applications, 2nd Edition, Prentice-Hall, New Jersey, 1981.

4. S. H. Crandall, W. D. Mark, Random Vibration in Mechanical Systems, Academic Press, New York, 1963.

5. H.S. Snay, "Model Tests and Scaling", NOLTR 63-257, Naval Ordnance Laboratory, White Oak, MD, December 1, 1964 (Unclassified) AD 357 501

6. J.L. Bogdanoff, J.E. Goldberg, and A.J. Schiff, "The Effect of Ground Transmission Time on the Response of Lone Structures", Report 8, Serial 1, Purdue Univ. Center of Applied Stochastics, Lafayette, IN, 1964.

7. N.E. Johnson, R.D. Galletly, "The Comparison of the Response of a Highway Bridge to Uniform Ground Shock and Moving Ground Excitation", The Shock and Vibration Bulletin, Bulletin 42, Part 2, January, 1972.

8. T.K. Hasselman, Review of "The Comparison of the Response of a Highway Bridge to Uniform Ground Shock and Moving Ground Excitation", The Shock and Vibration Digest, Volume 5, No. 2, February, 1973.

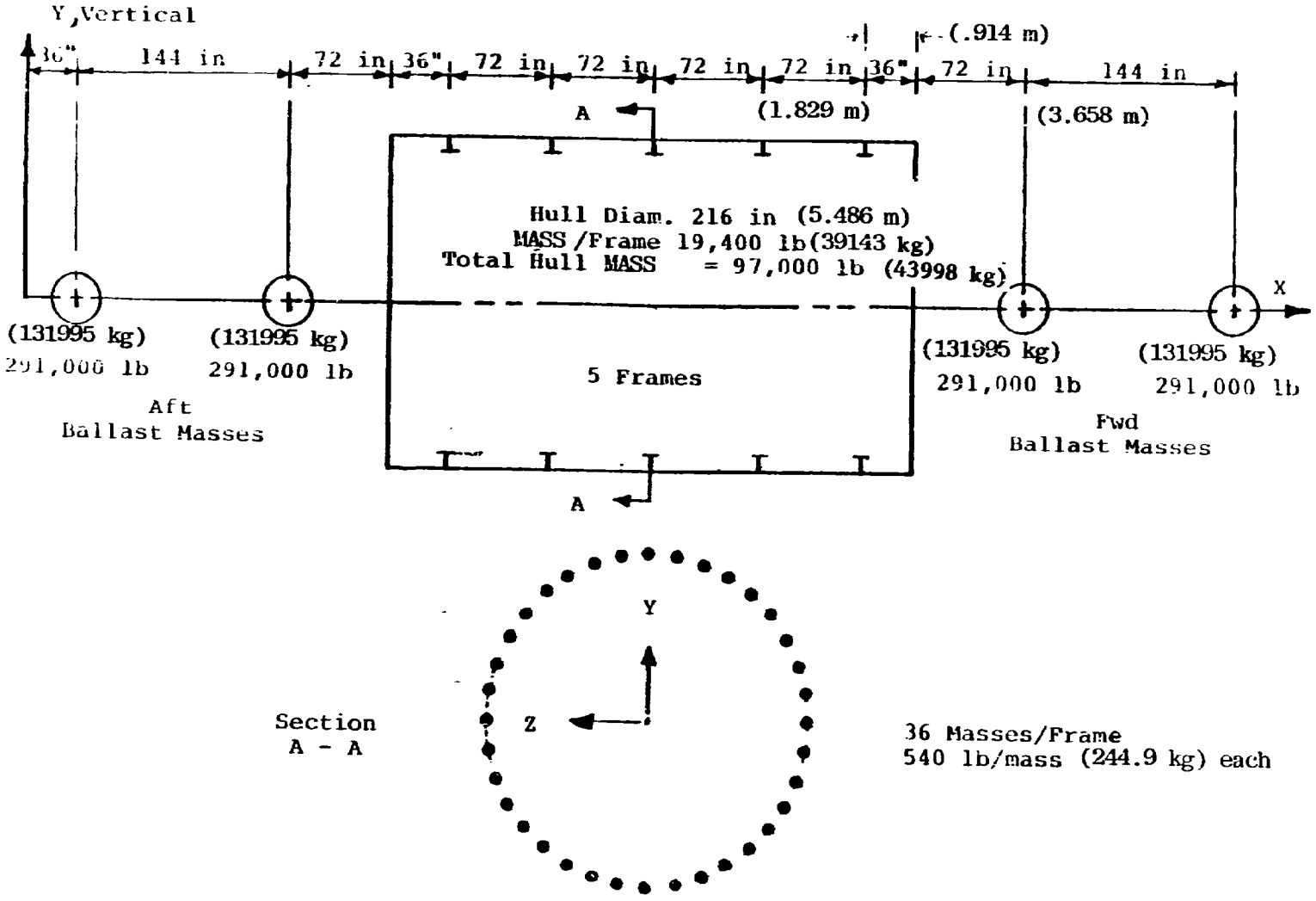

Fig. 1 — VGSM Model

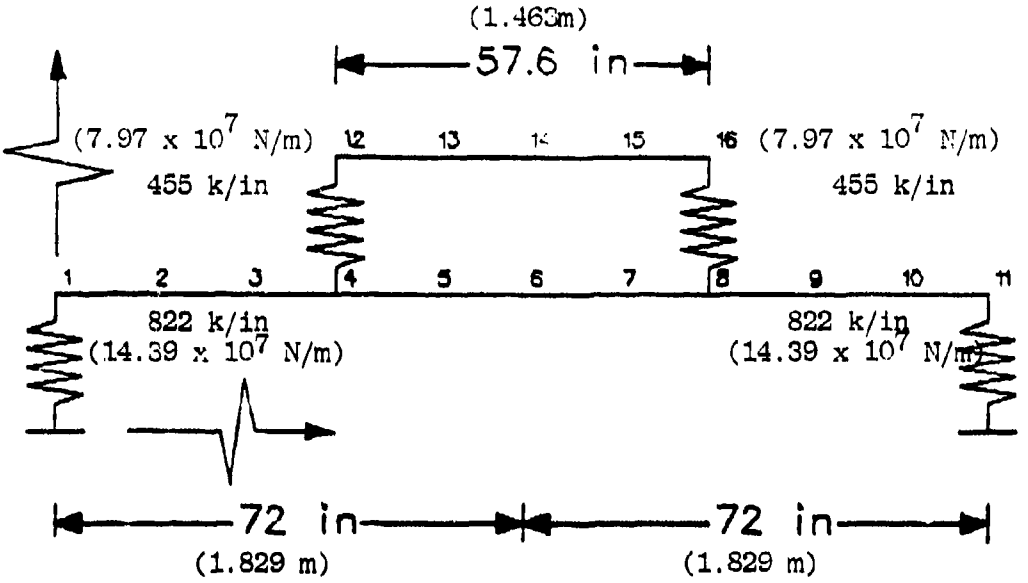

CROSS SECTION MOMENTS OF INERTIA

Upper Beam: 200 in^4 (8.325 x 10^{-5} m^4)
Lower Beam: 1200 in^4 (49.948 x 10^{-5} m^4)

ELASTIC MODULUS: 30 x 10^6 psi (206843 MPa)

MASS VALUES BY MASS NUMBER: lb - sec^2/in or (kg)

1	0.5 (87.5)	9	1.0 (175)
2	1.0 (175)	10	1.0 (175)
3	1.0 (175)	11	0.5 (87.5)
4	2.0 (350)	12	2.0 (350)
5	1.0 (175)	13	3.0 (525)
6	1.0 (175)	14	4.0 (700)
7	1.0 (175)	15	3.0 (525)
8	2.0 (350)	16	2.0 (350)

TOTAL MASS: 26.0 lb-sec^2/in (4553.3 kg)
TOTAL WEIGHT: 10038 lb (44652 N)

Fig. 2 — Internal equipment model

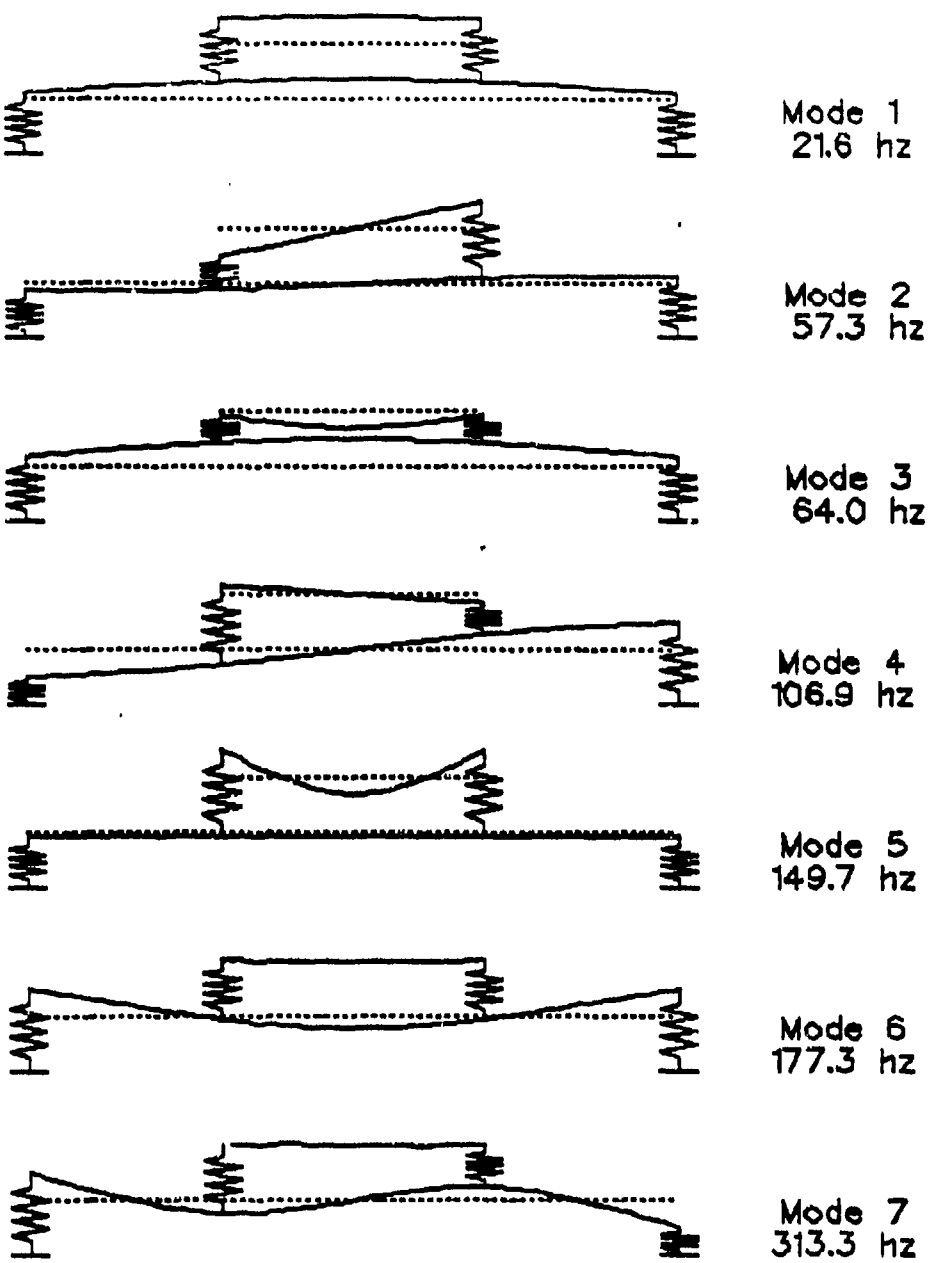

Fig. 3 — Fixed base modes and frequencies of equipment

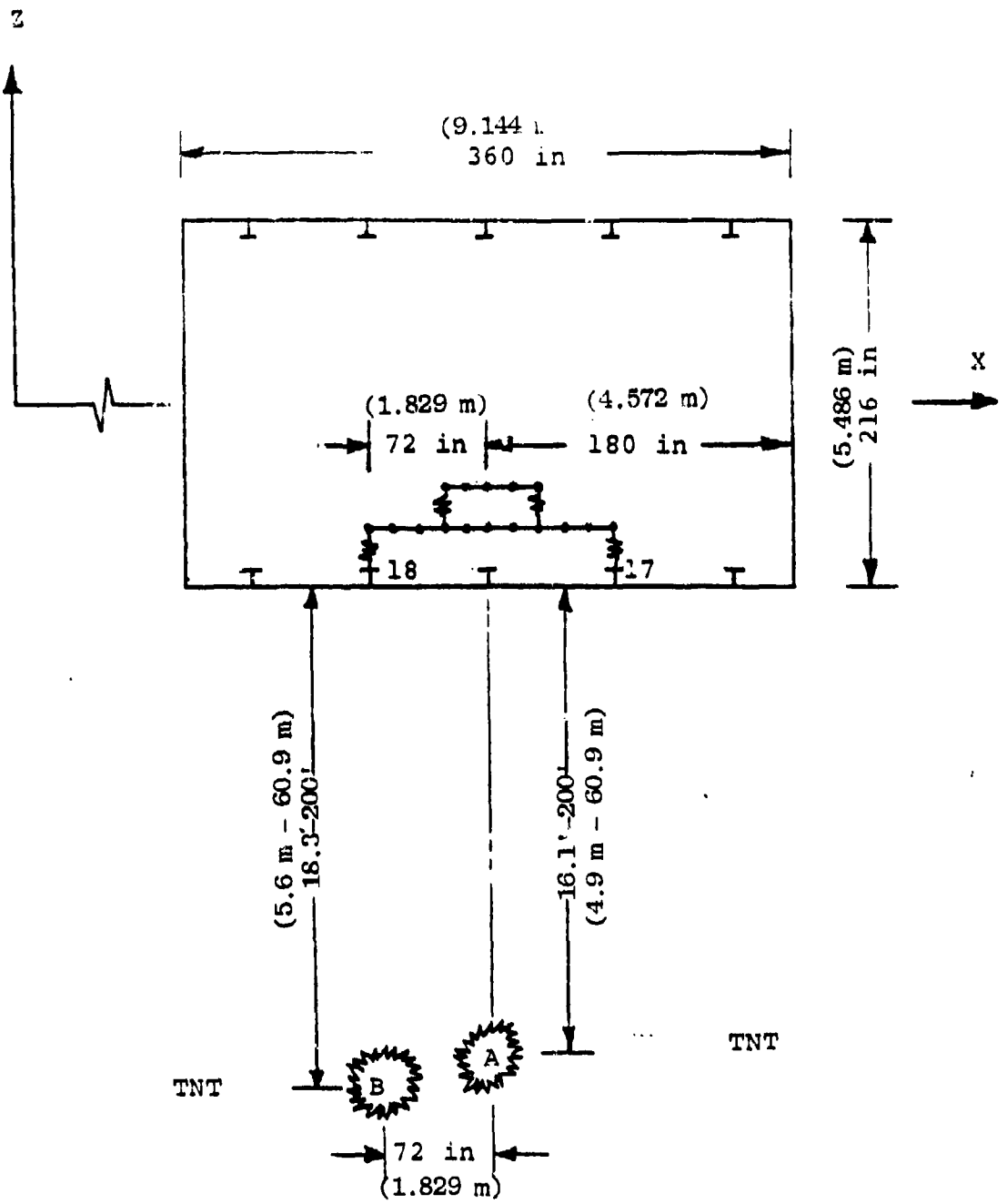

Fig. 4 — Simulated explosion geometries

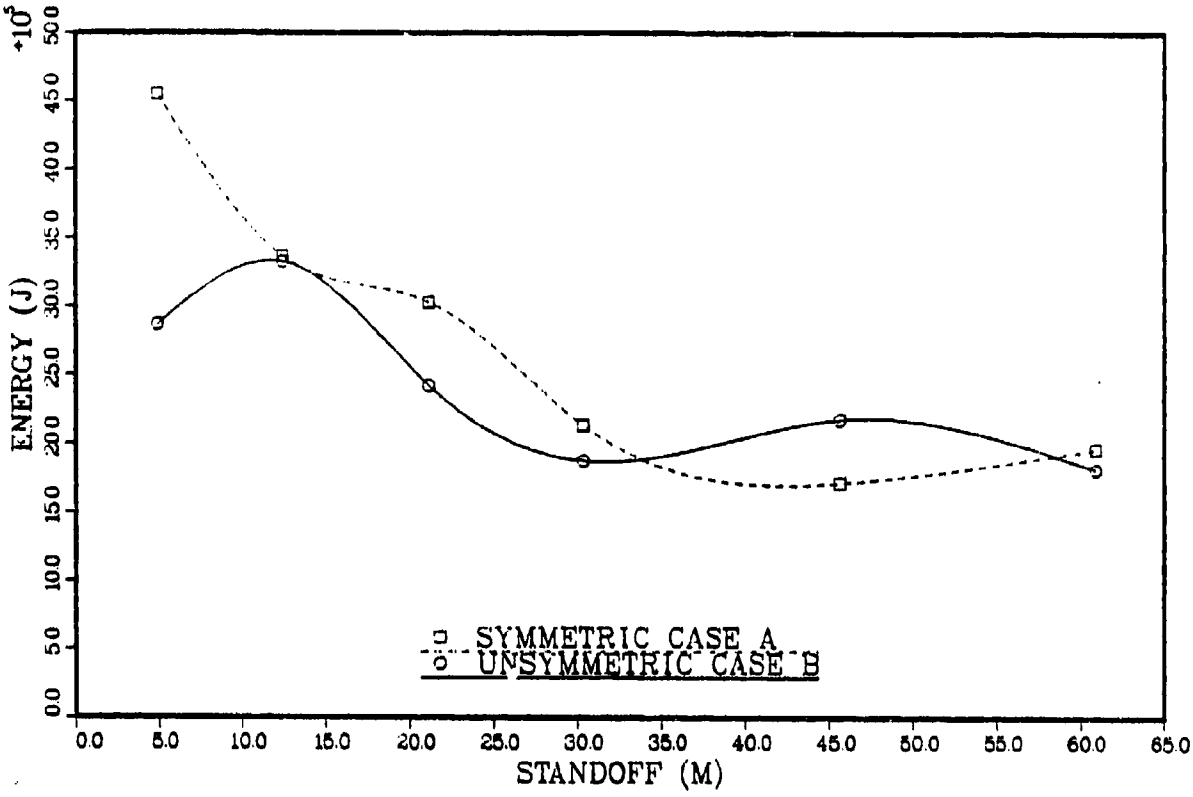

Fig. 5 — Kinetic energy

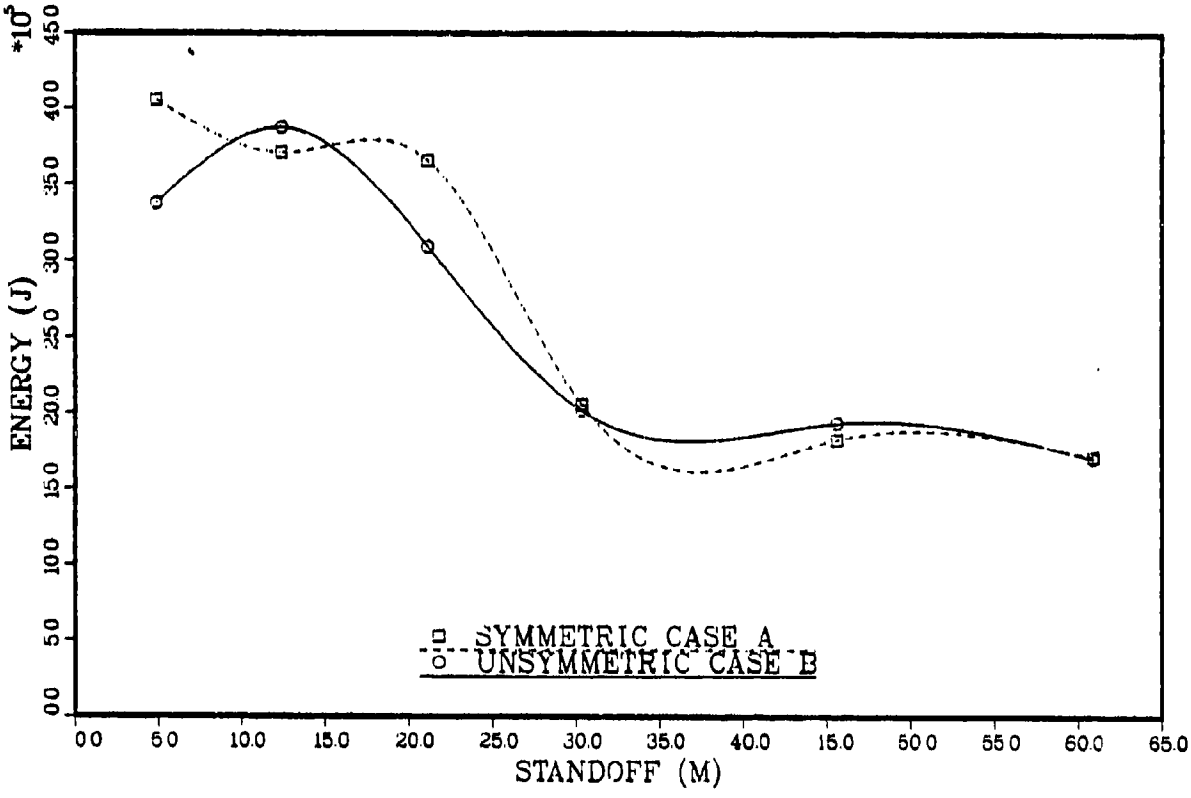

Fig. 6 — Potential energy

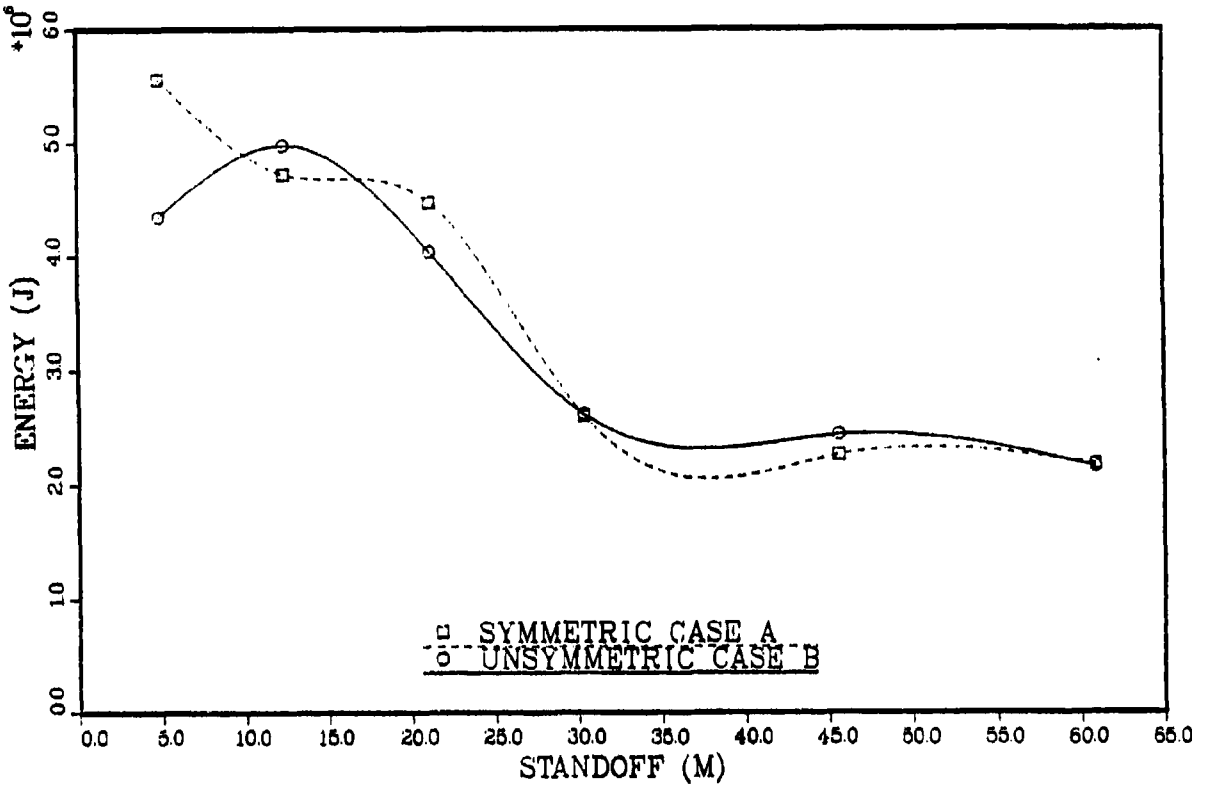

Fig. 7 -- Total energy

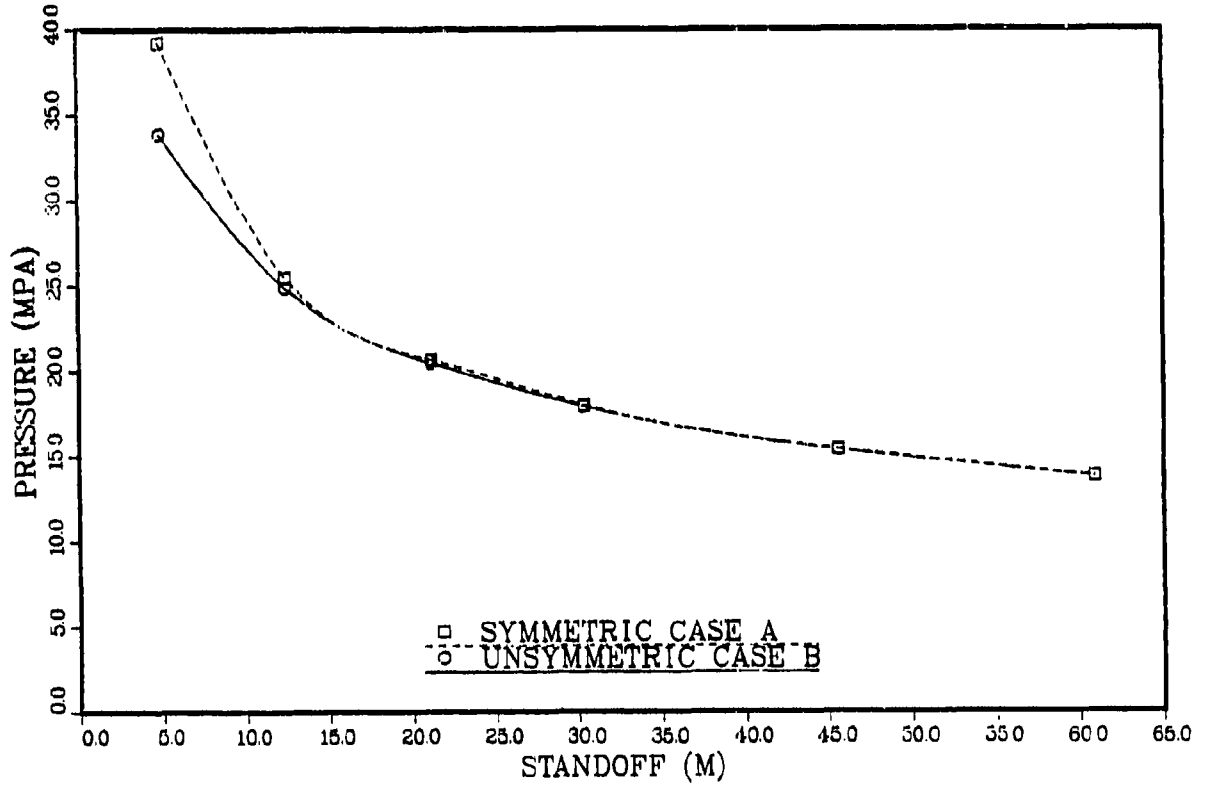

Fig. 8 — Overpressure of explosion at hull

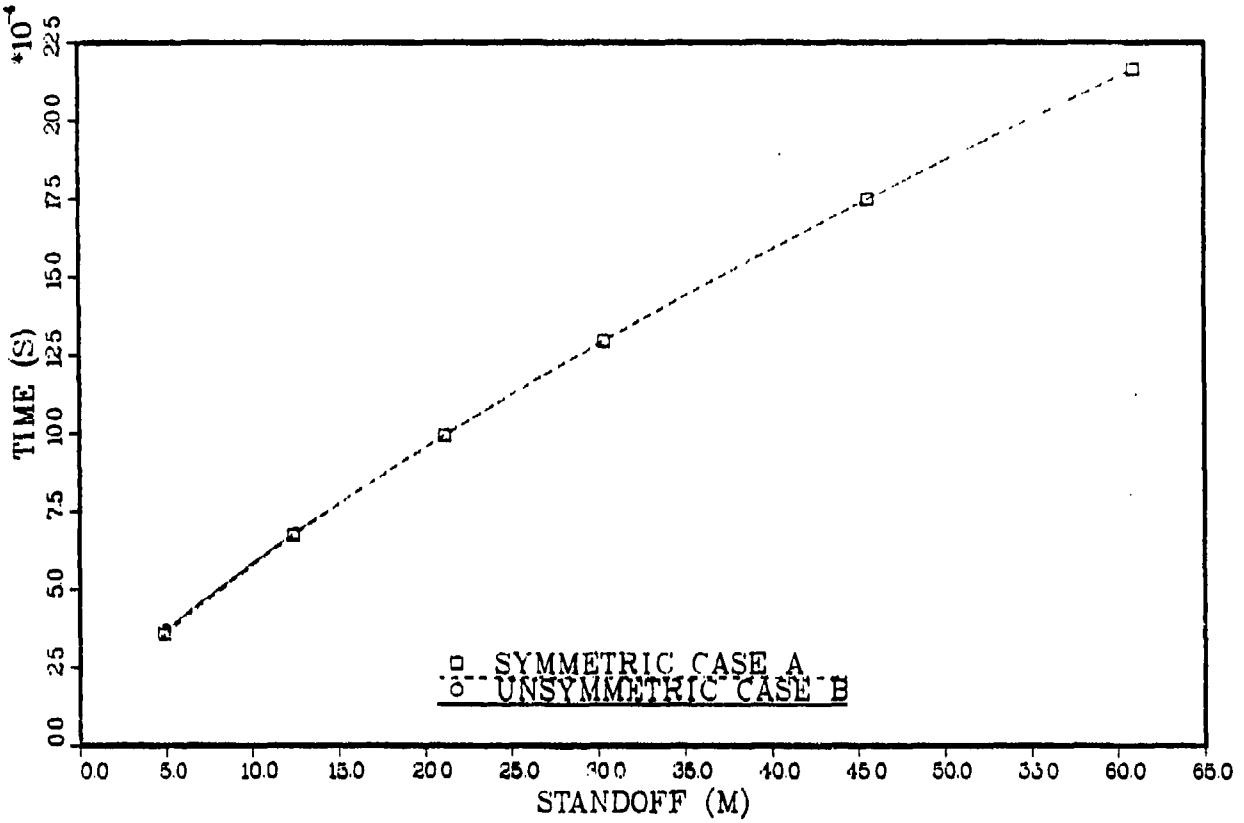

Fig. 9 — Time constant of explosion at hull

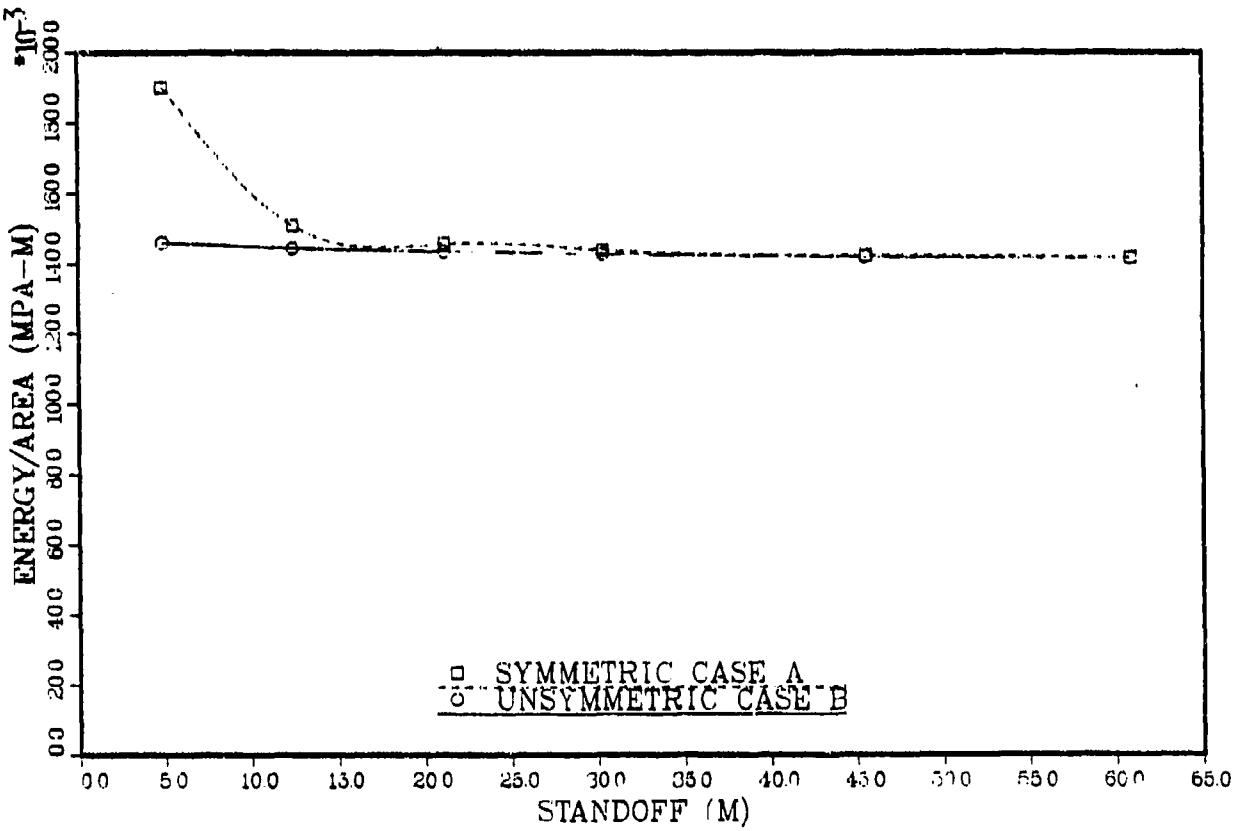

Fig. 10 — Energy/area of explosion at hull

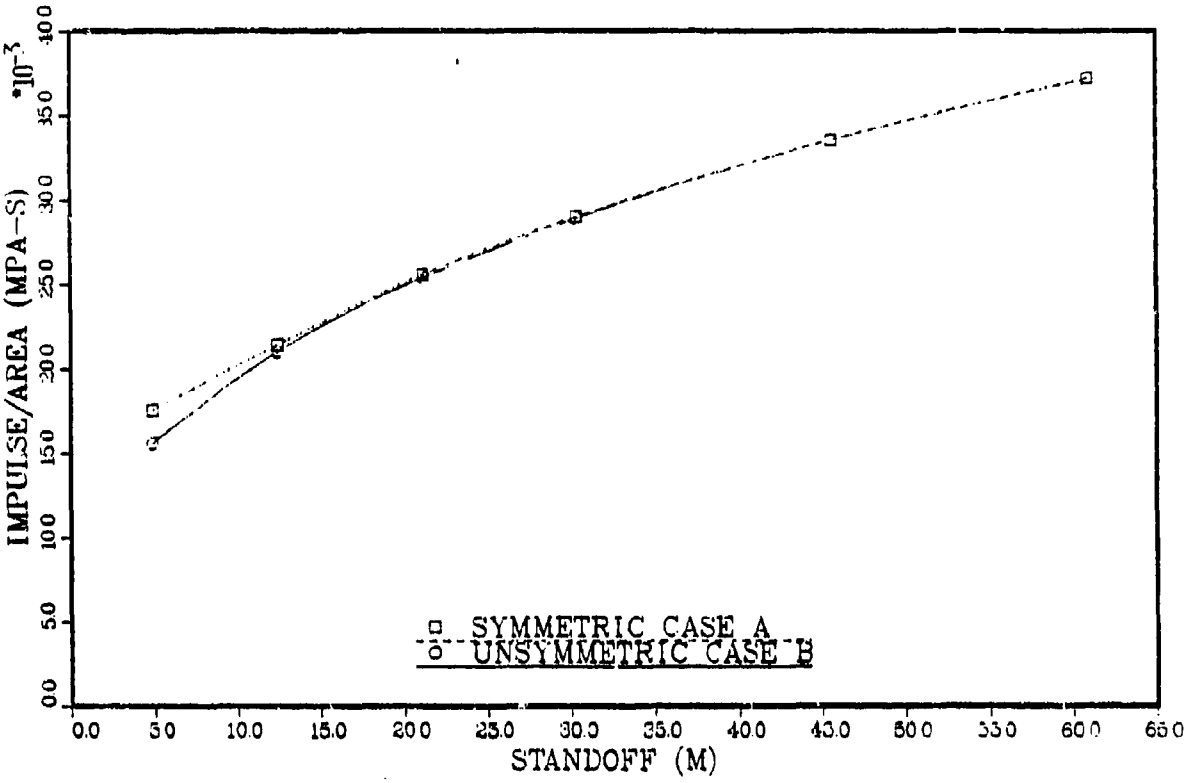

Fig. 11 — Impulse/area of explosion at hull

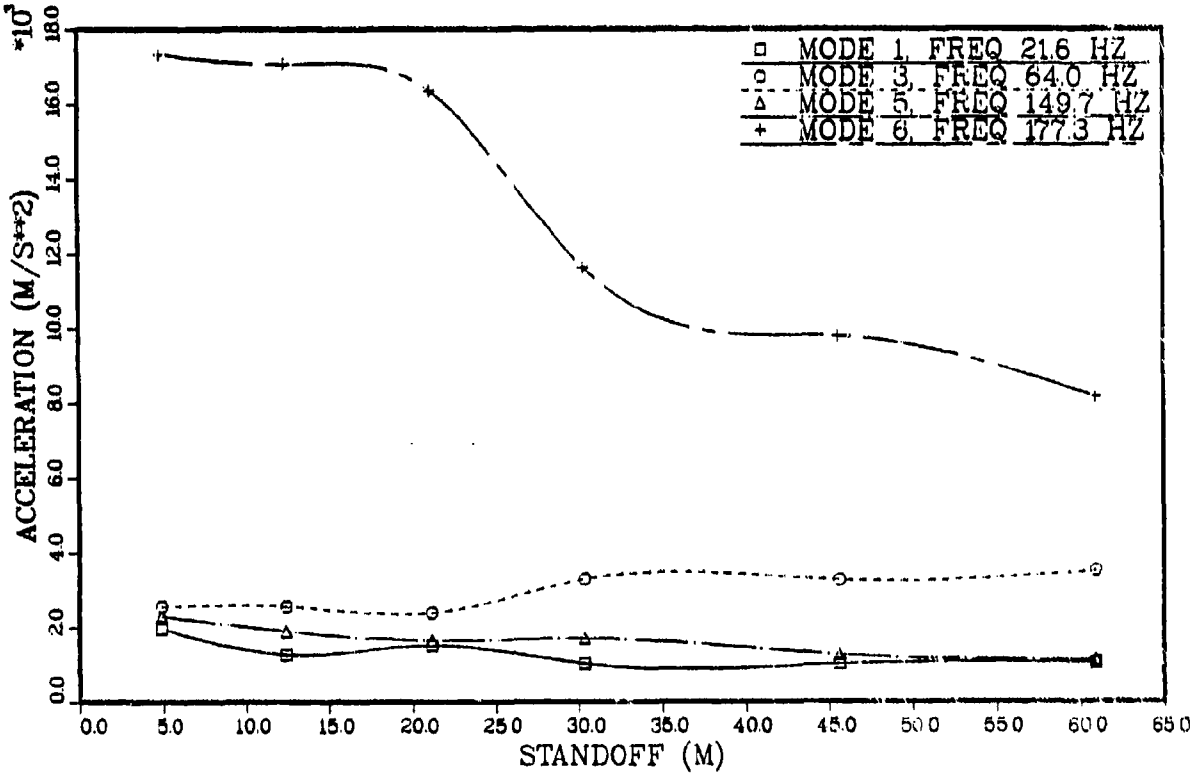

Fig. 12 — Modal amplitudes for symmetric Case A

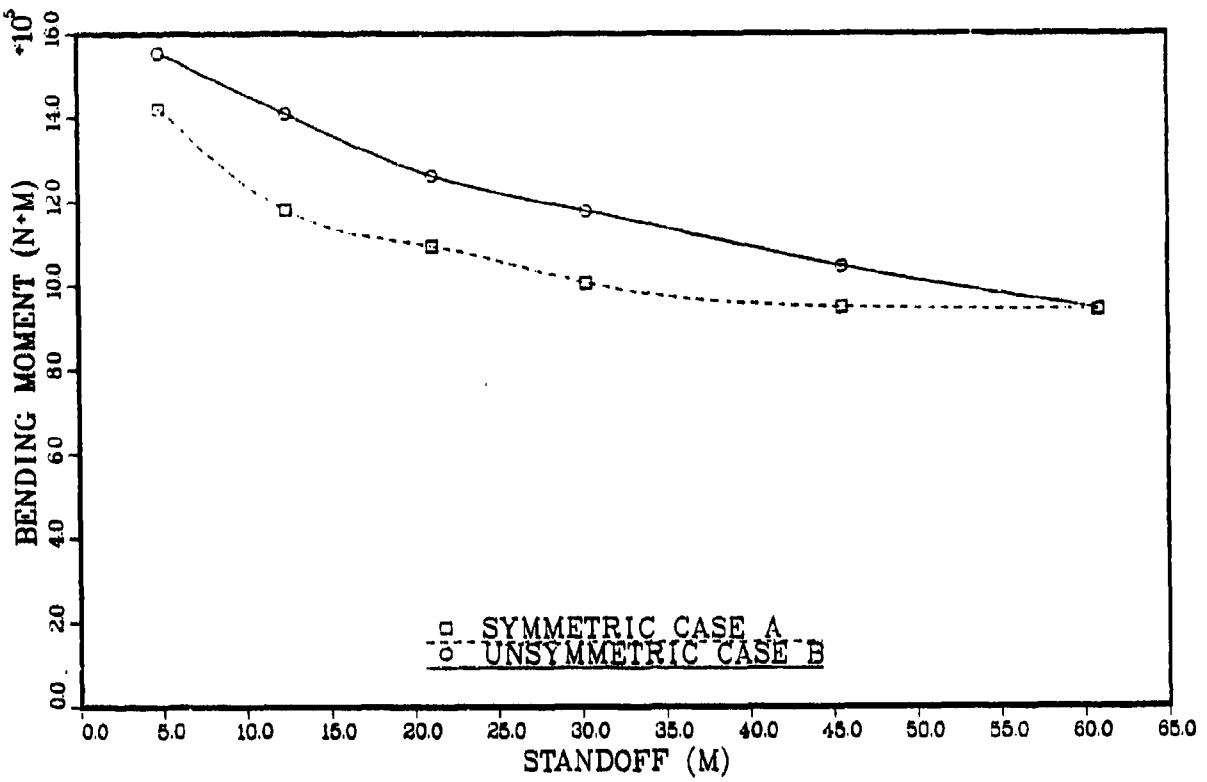

Fig. 13 — Bending moment #1

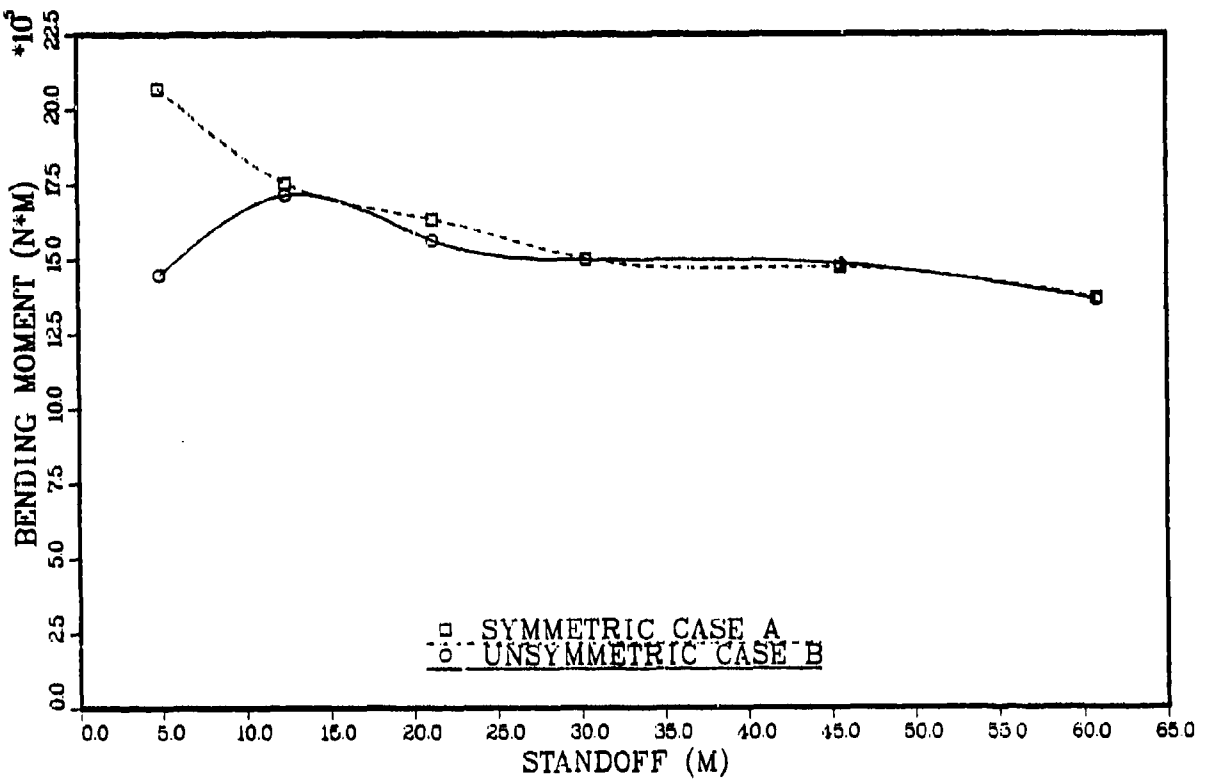

Fig. 14 — Bending moment #2

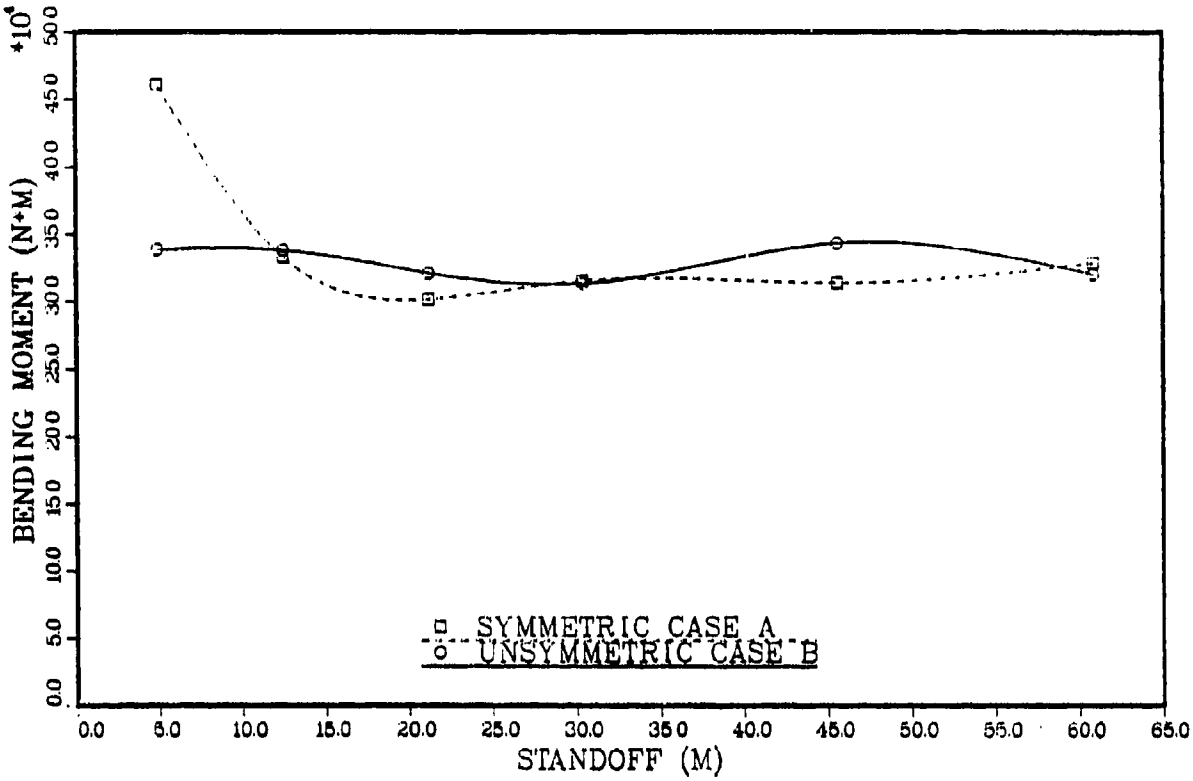

Fig. 15 — Bending moment #3

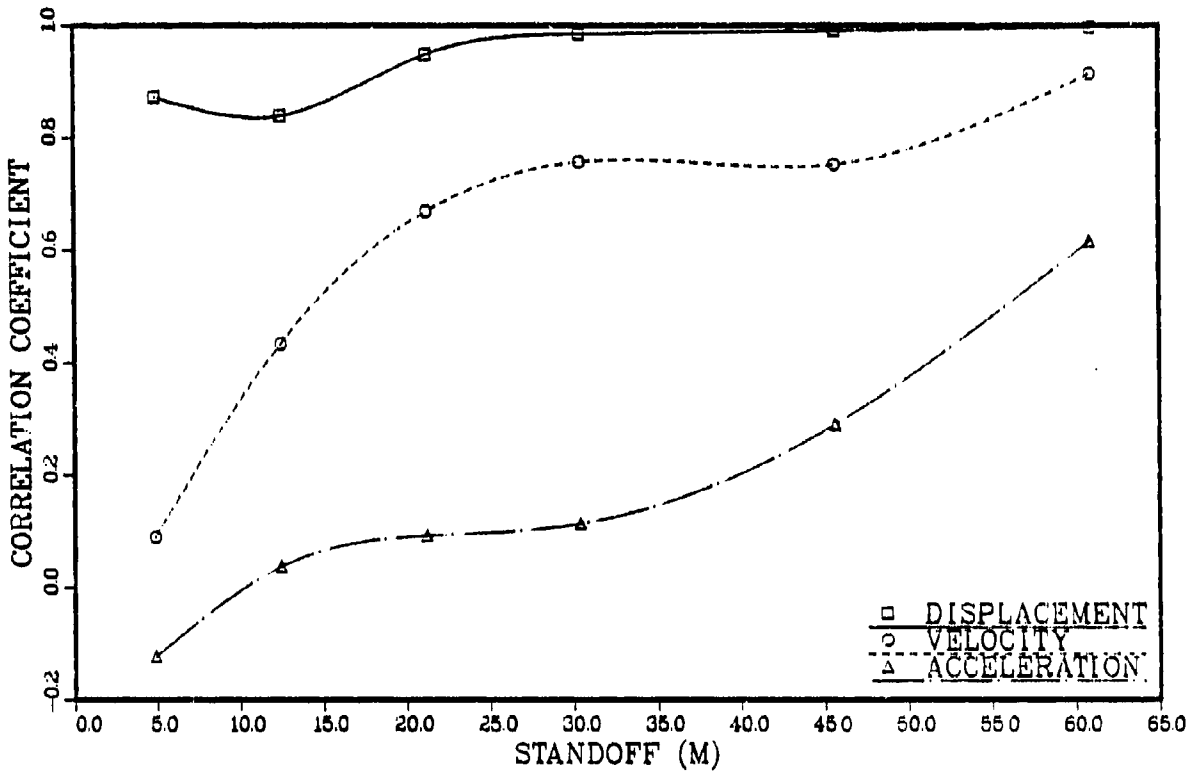

Fig. 16 — Correlation of foundation motions, Case B

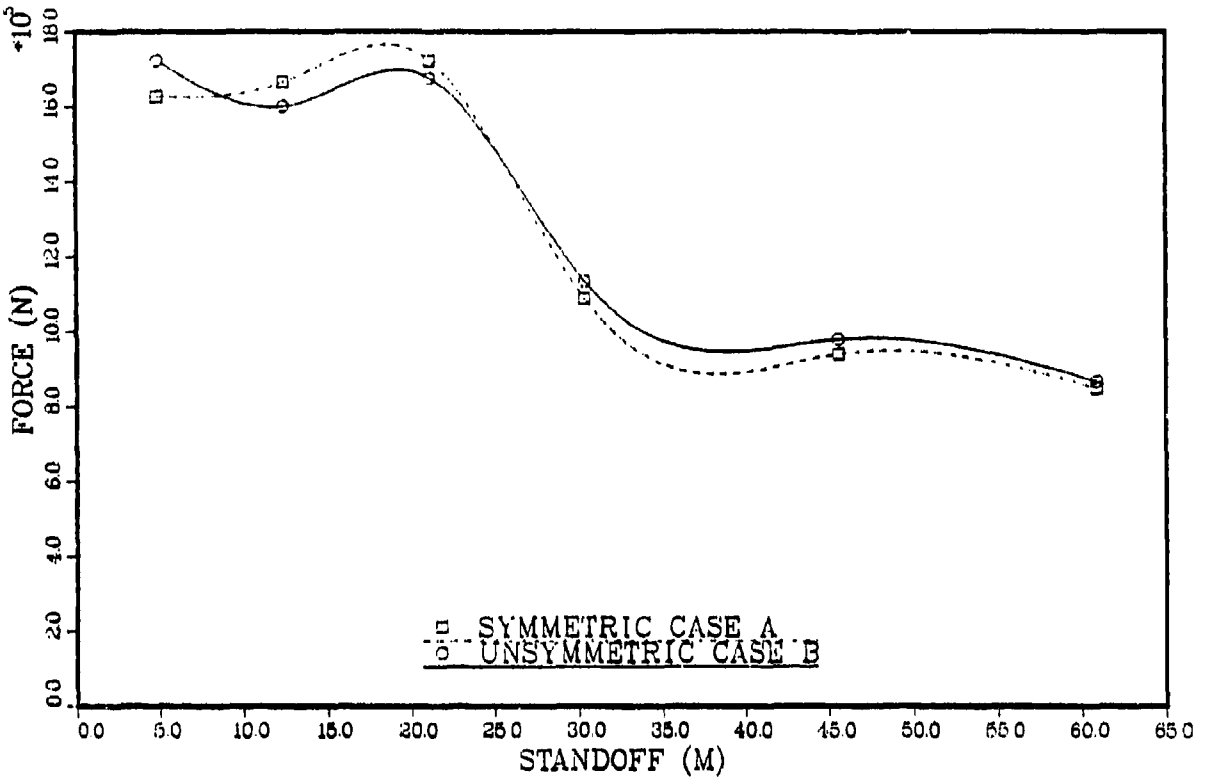

Fig. 17 — Force in spring nodes 18 to 11

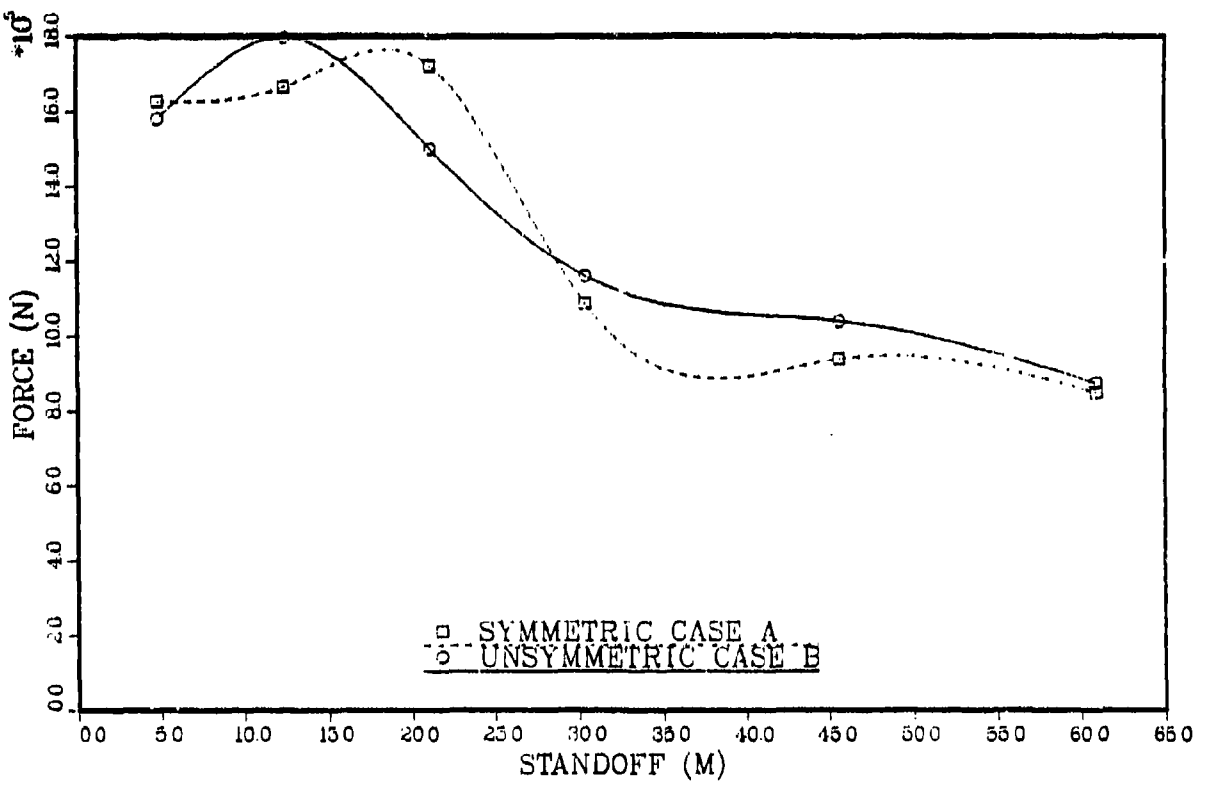

Fig. 18 — Force in spring nodes 17 to 1

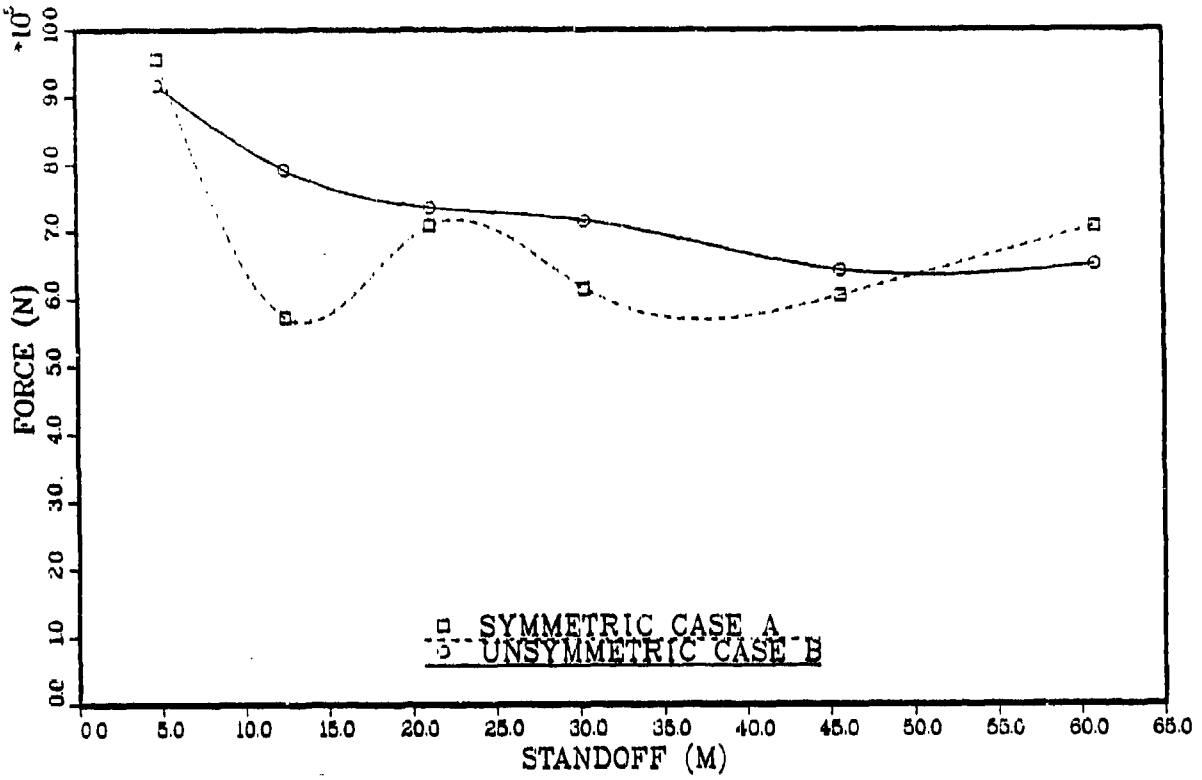

Fig. 19 — Force in spring nodes 4 to 12

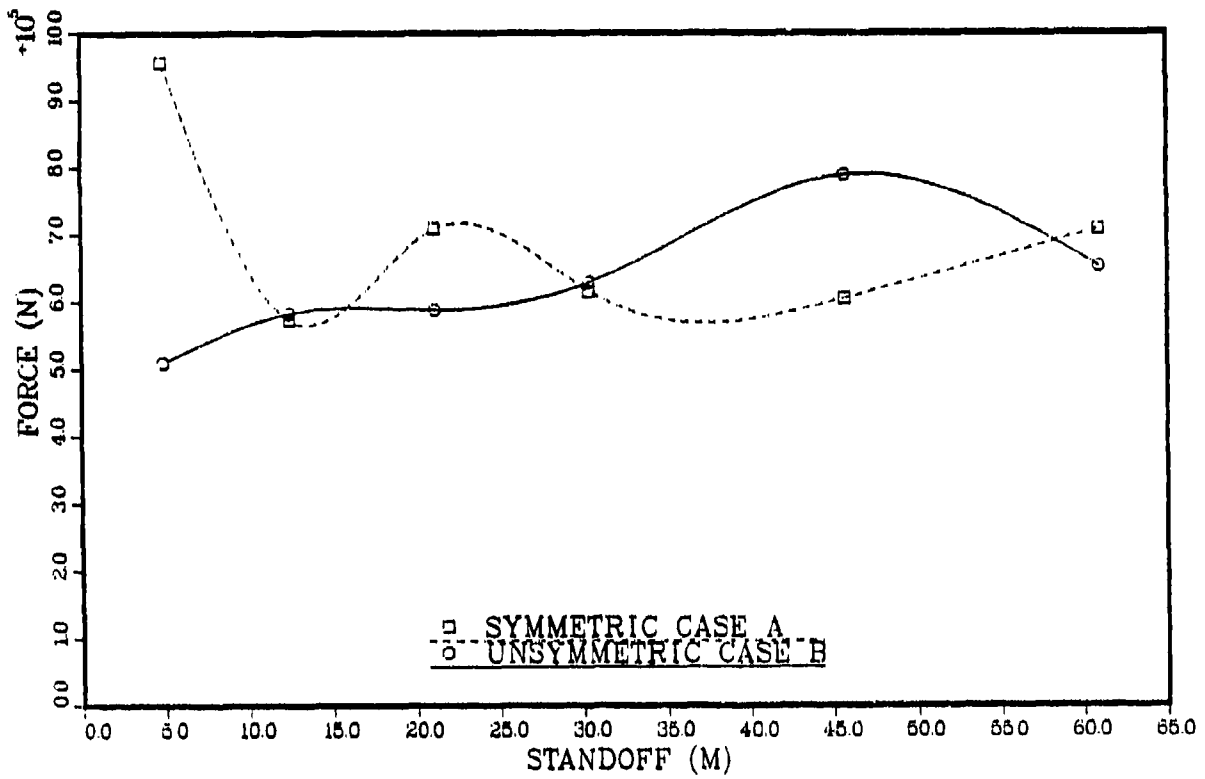

Fig. 20 — Force in spring nodes 8 to 16

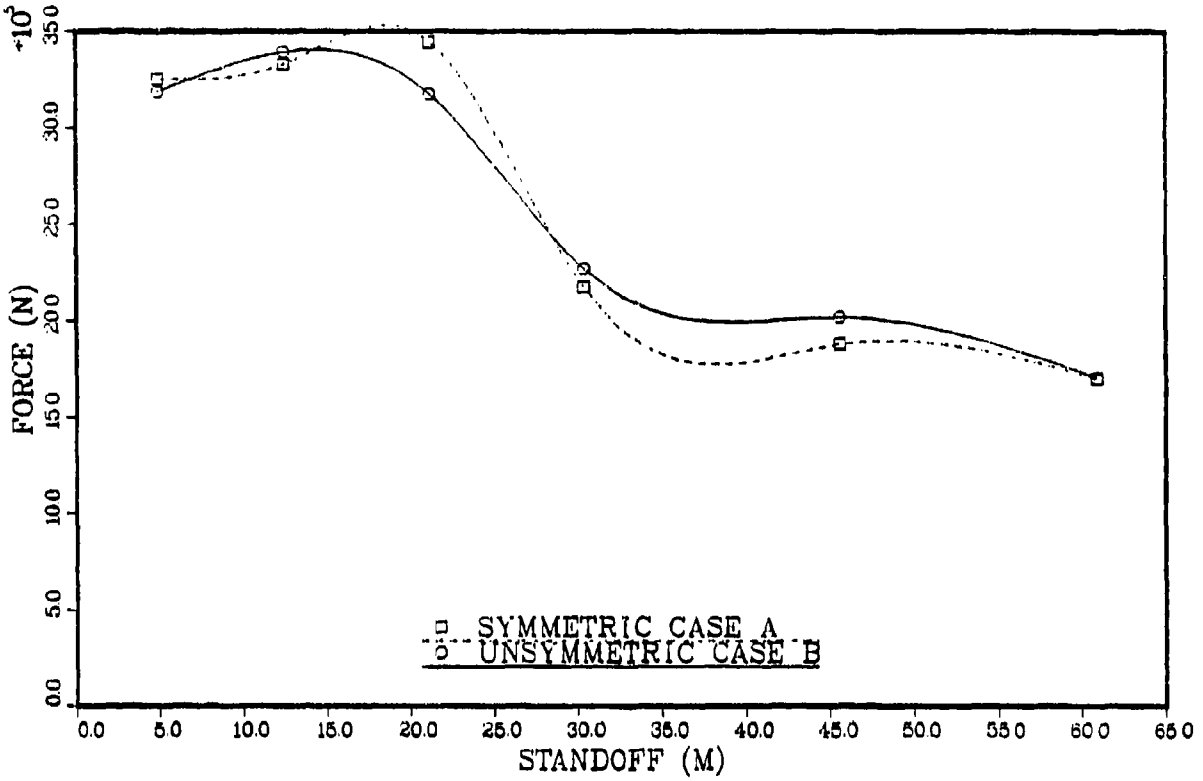

Fig. 21 — Sum of springs supporting equipment

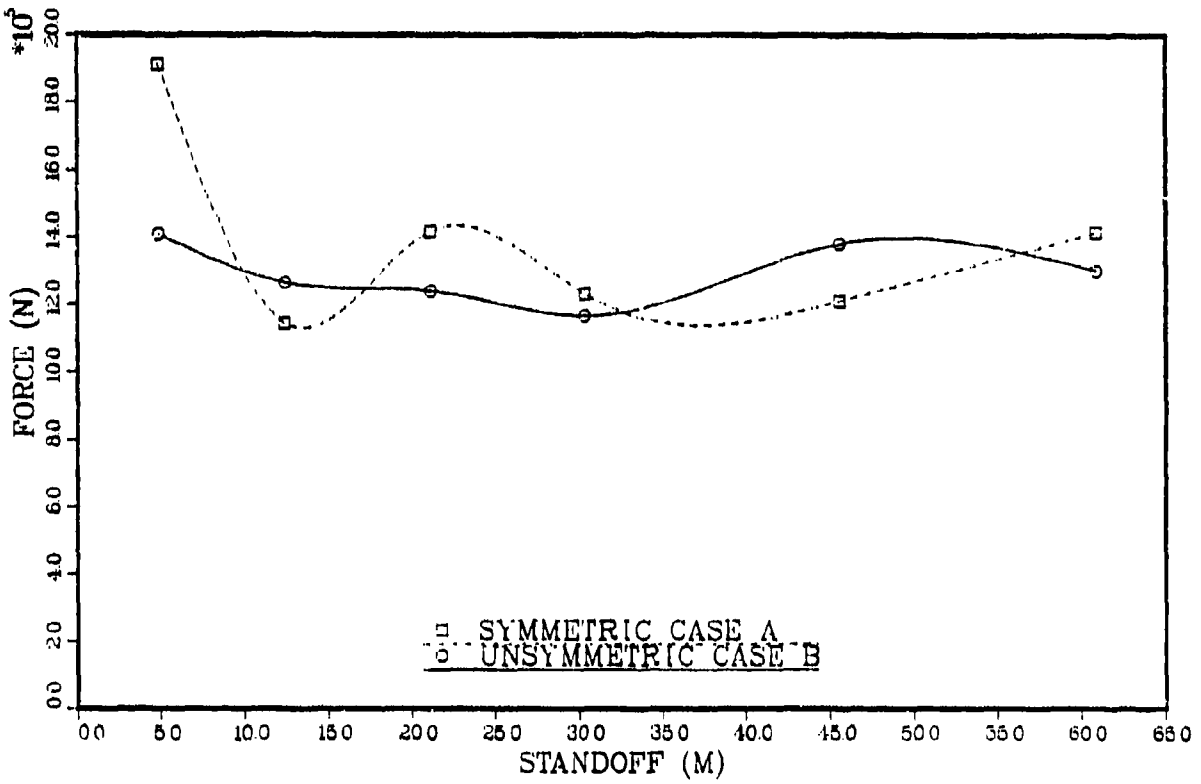

Fig. 22 — Sum of springs supporting upper beam

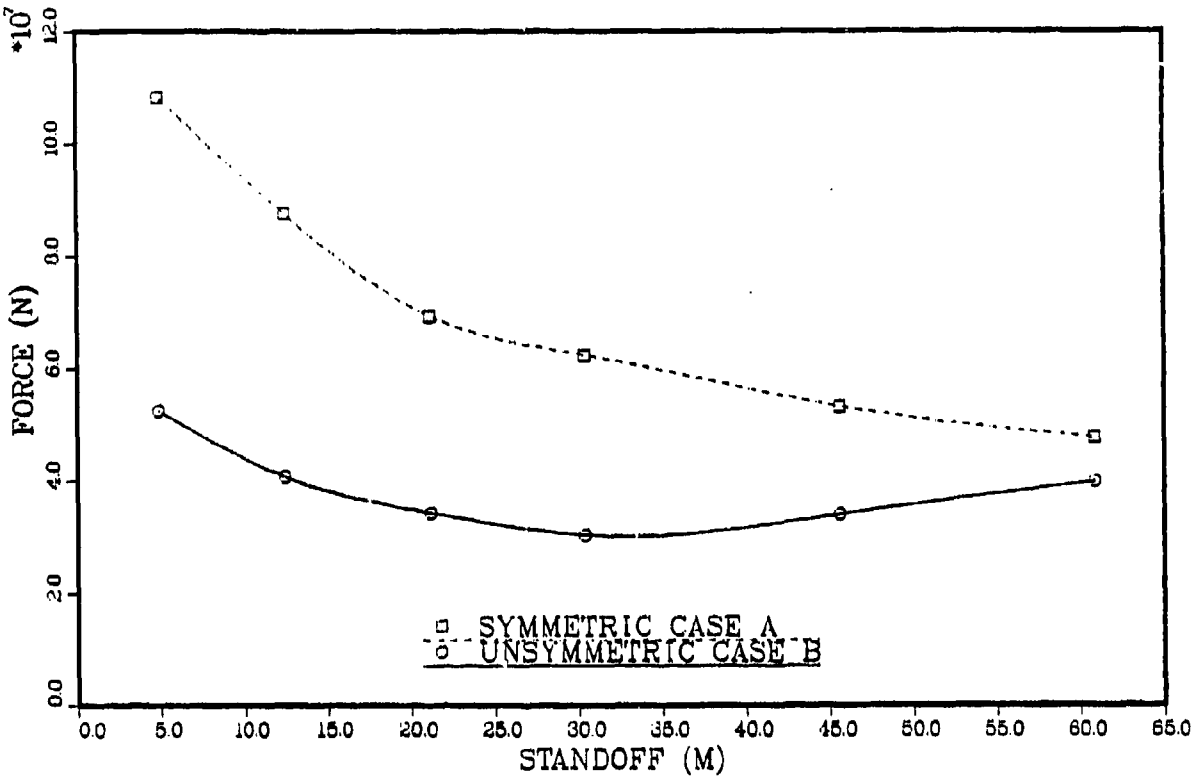

Fig. 23 — Sum of all dynamic loads on masses

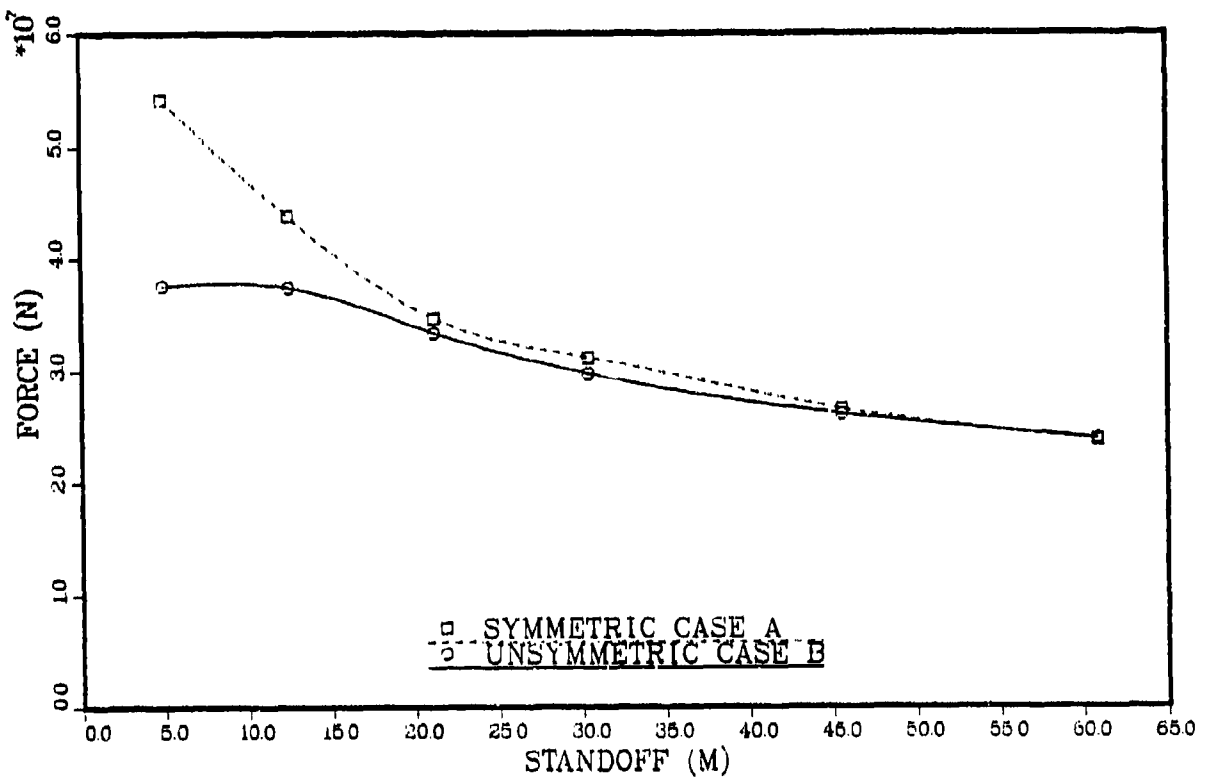

Fig. 24 — Reaction at 17

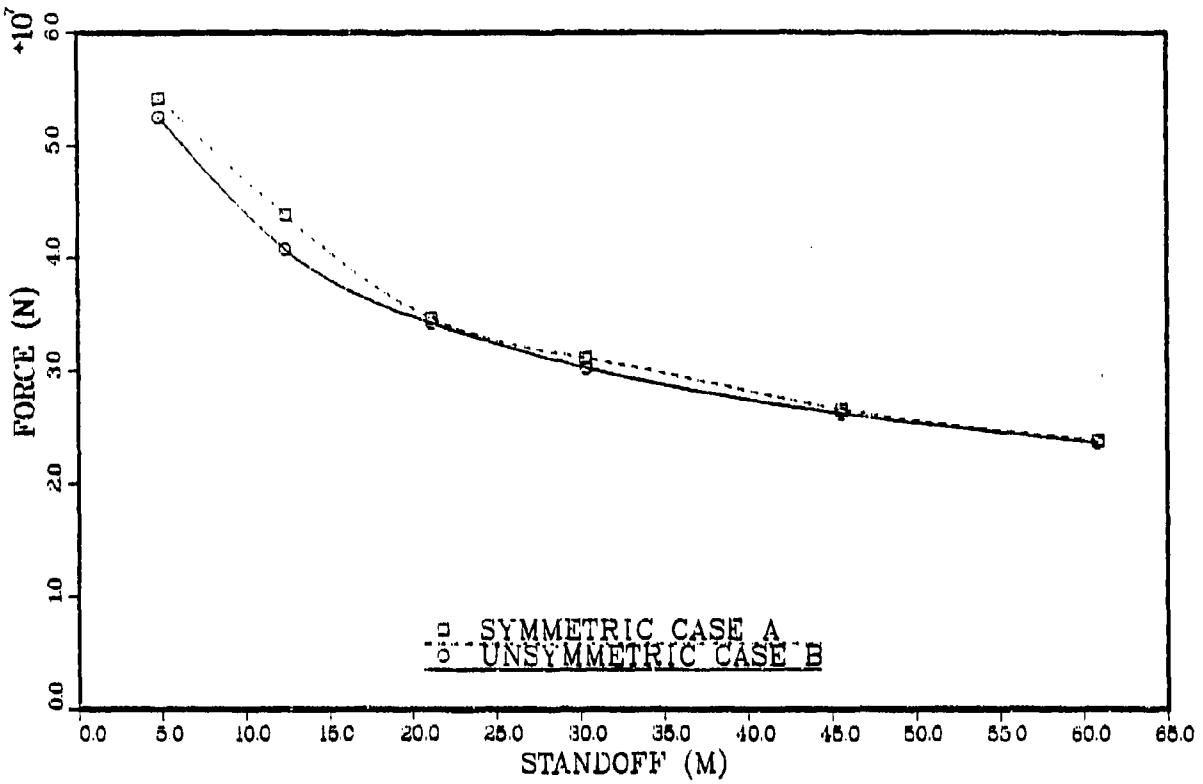

Fig. 25 — Reaction at 18

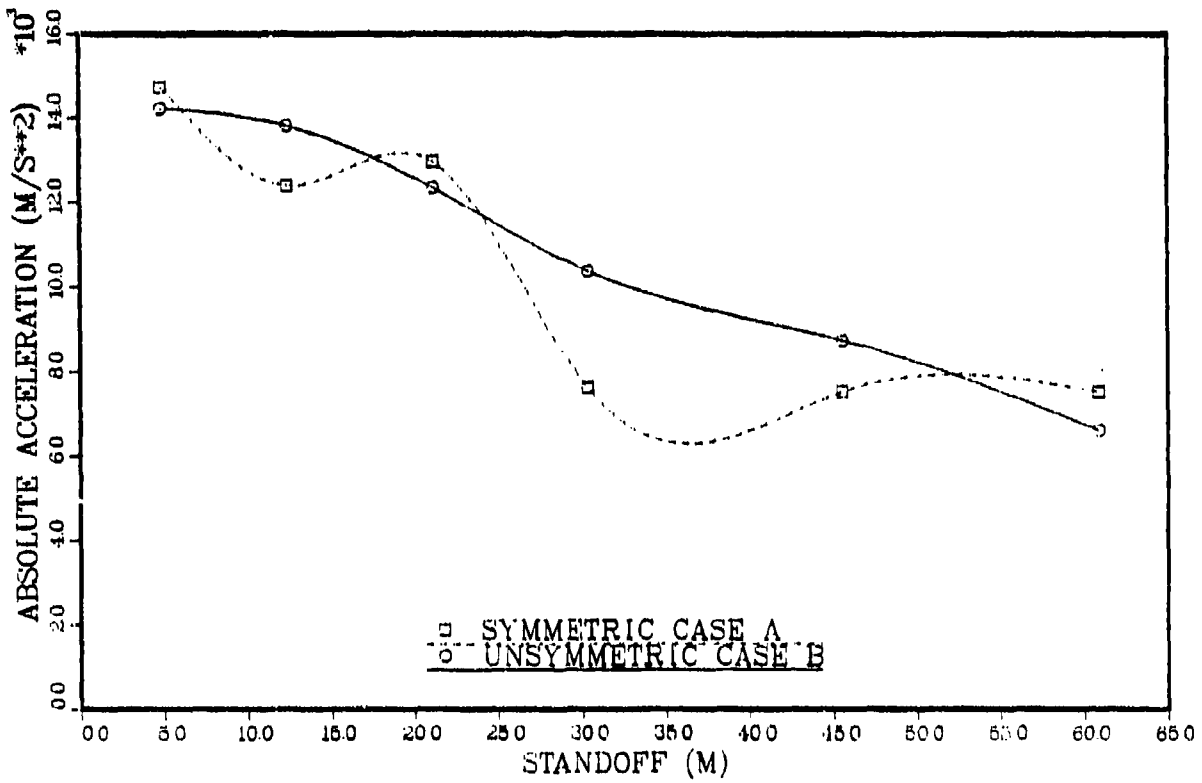

Fig. 26 — Acceleration at mass #1

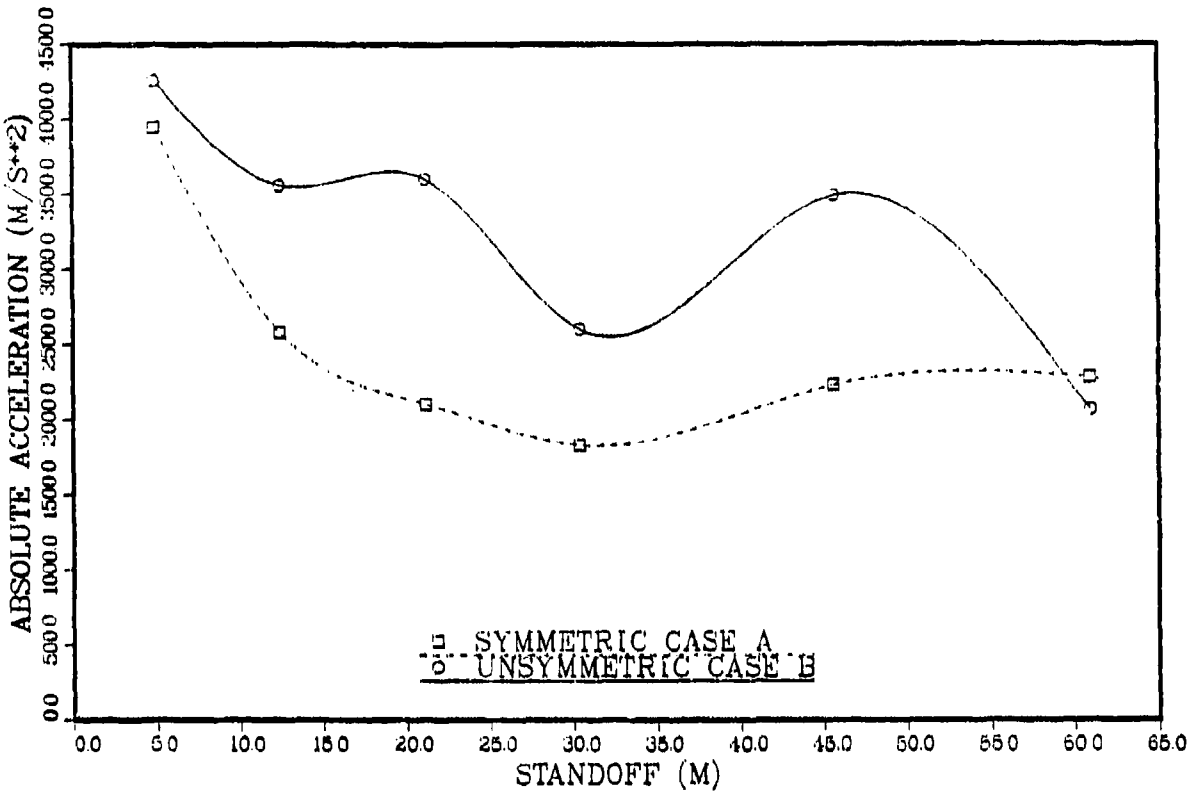

Fig. 27 — Acceleration at mass #4

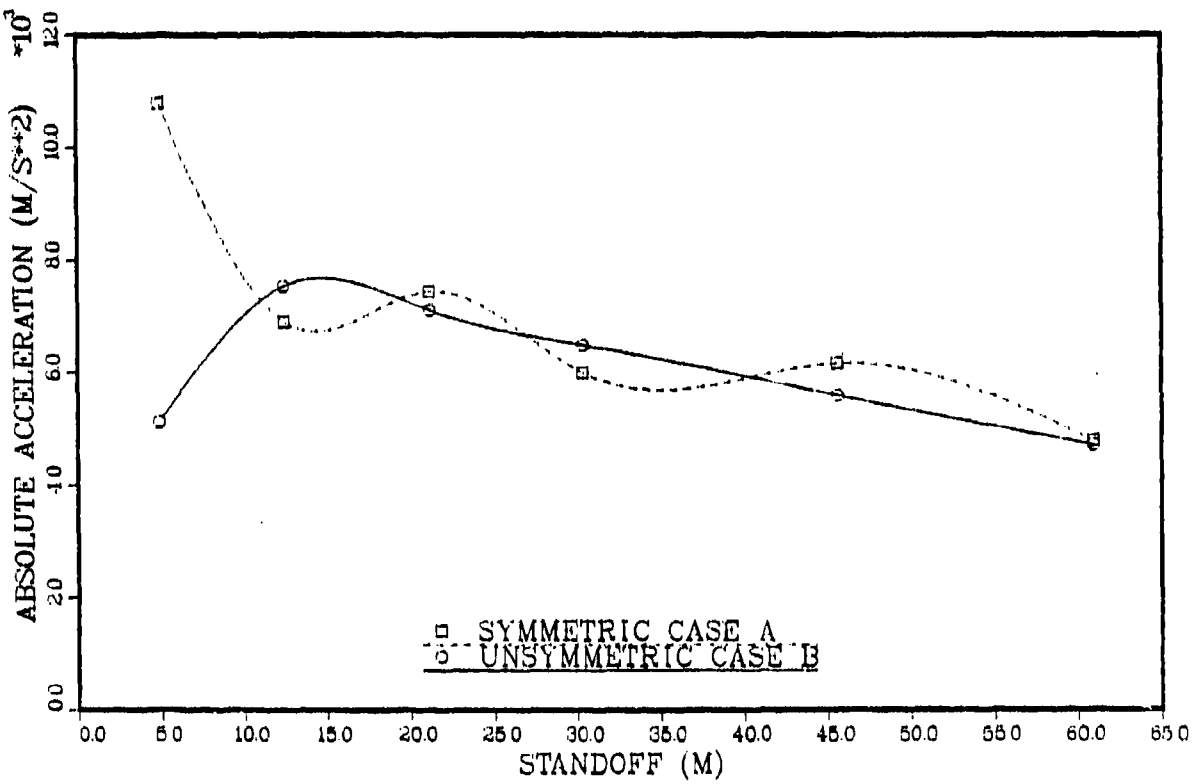

Fig. 28 — Acceleration at mass #6

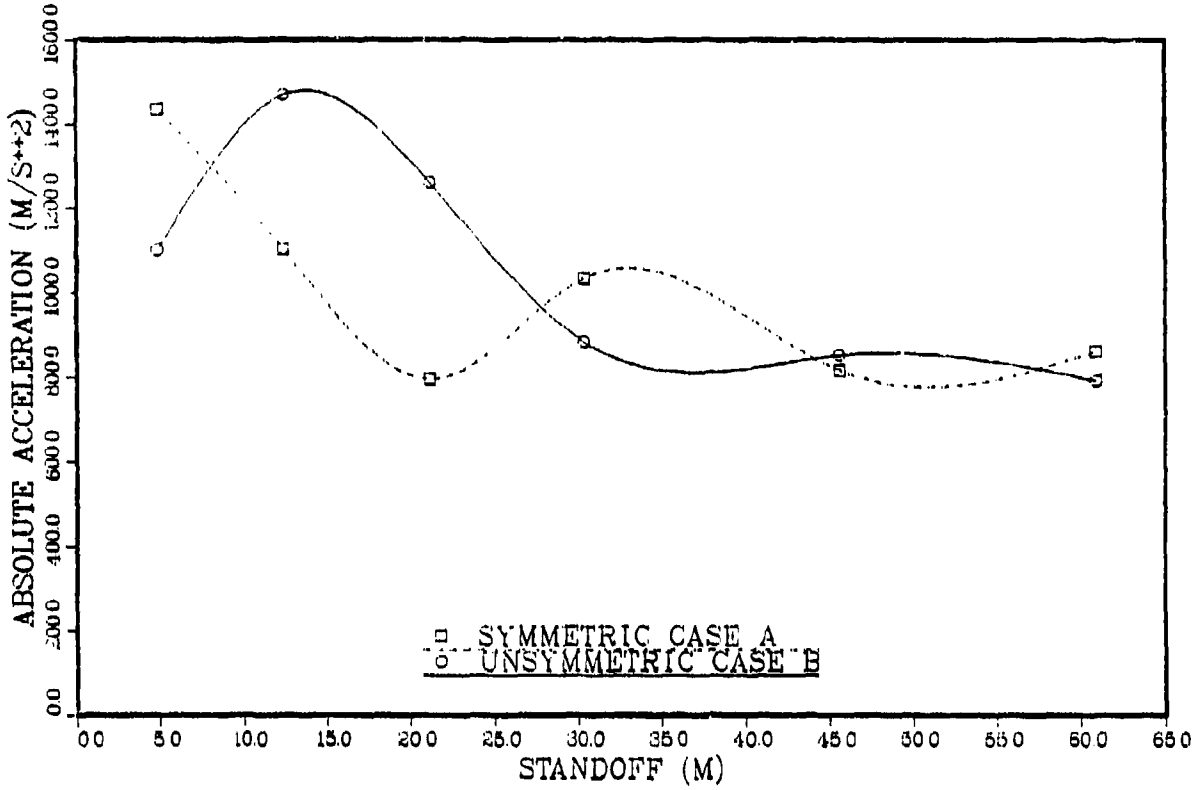

Fig. 29 — Acceleration at mass #12

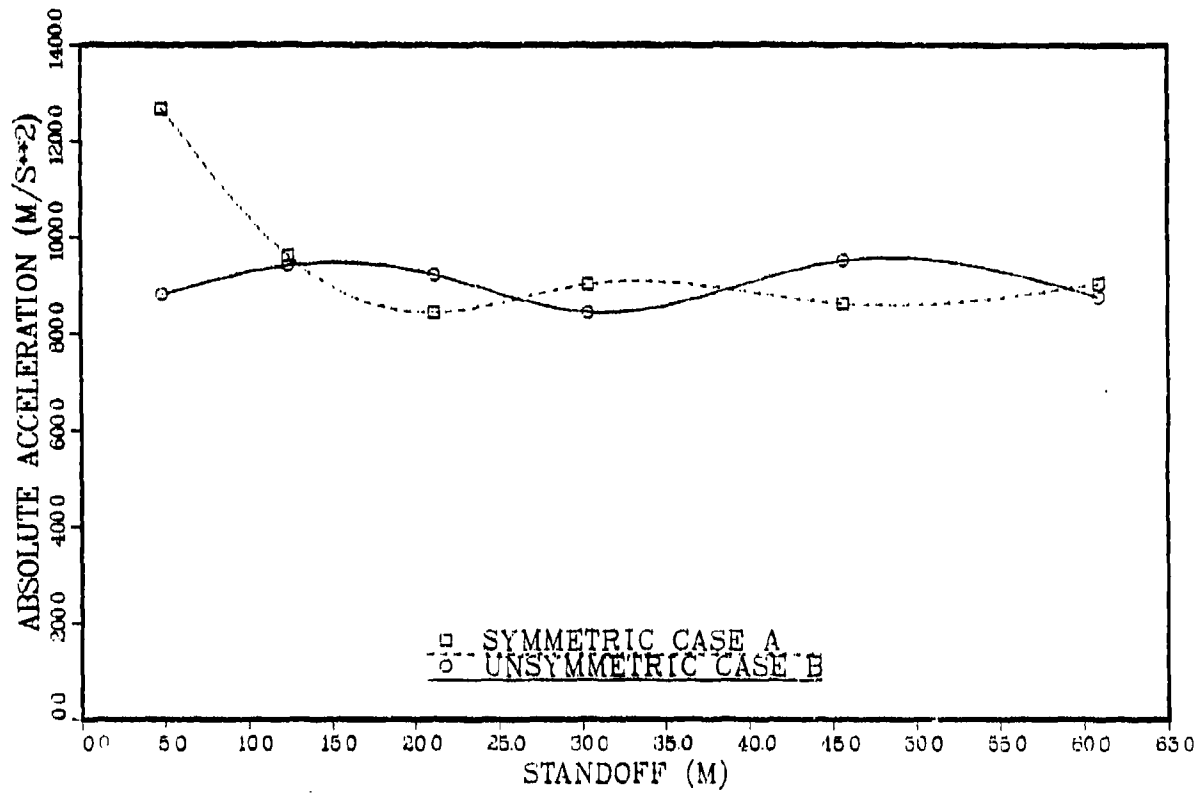

Fig. 30 — Acceleration at mass #14